IEEE Access
Multidisciplinary | Rapid Review | Open Access Journal

Received September 12, 2018, accepted October 15, 2018, date of publication October 18, 2018,
date of current version November 14, 2018.

*Digital Object Identifier 10.1109/ACCESS.2018.2876718*

# Hybrid Timescale Dispatch Hierarchy for Combined Heat and Power System Considering the Thermal Inertia of Heat Sector

**SHUAI YAO, (Student Member, IEEE), WEI GU, (Senior Member, IEEE), SUYANG ZHOU, SHUAI LU, CHENYU WU, AND GUANGSHENG PAN, (Student Member, IEEE)**
School of Electrical Engineering, Southeast University, Nanjing 210096, China

Corresponding author: Wei Gu (wgu@seu.edu.cn)

This work was supported by the National Natural Science Foundation of China under Grant 51477029.

**ABSTRACT** To better accommodate the uncertainty introduced by renewables and loads, a hybrid timescale dispatch hierarchy for the combined heat and power system is constructed in this paper, which coordinates the stages of day-ahead dispatch, intraday rolling dispatch, real-time dispatch, and automatic generation control to decompose the uncertainty step by step. Considering the different features of heat and power sector, heating units should have different dispatch intervals from power units in each dispatch stage. Therefore, a method considering the extra operation and maintenance costs of frequent adjustment, the operation modes of district heating network (DHN), and the heat storage capacity of buildings is developed to determine the optimal dispatch interval of each unit. The thermal inertia of heat sector is also integrated into the dispatch model to improve wind power consumption. The model of buildings directly links the indoor temperature with the temperature of supplied water and can be easily applied to determine the state of DHN. Results of the case study validate the feasibility and effectiveness of the proposed dispatch method in terms of enhancing the economical efficiency and wind power consumption.

**INDEX TERMS** Combined heat and power, hybrid timescale dispatch, dispatch interval, thermal inertia, district heating network, wind power.

## NOMENCLATURE

*Indices and Index Sets:*

| | |
|---|---|
| $S^i$ | Set of nodes connecting node $i$ directly |
| $S^{\mathrm{p}}$ | Set of pipelines |
| $S_k^{\mathrm{p}}$ | Set of pipelines from the first to the $k$th one |
| $S^{\mathrm{bus}}/S^{\mathrm{gen}}$ | Set of all buses/generators in the DHN |
| $S^{\mathrm{load}}$ | Set of all loads in the system |

*Variables:*

| | |
|---|---|
| $P^{\mathrm{CHP}}$ | Electric power output of CHP unit |
| $m^{\mathrm{s}}/m^{\mathrm{w}}$ | Mass flow rate of steam/water |
| $f^{\mathrm{CHP}}$ | Operational coal use of CHP unit |
| $Q_{\mathrm{P}}^{\mathrm{HX}}/Q_{\mathrm{S}}^{\mathrm{HX}}$ | Heat power exchanged by primary/ secondary heat exchanger |
| $T^{\mathrm{stm}}$ | Temperature of steam |
| $T^{\mathrm{w,h}}/T^{\mathrm{w,c}}$ | Temperature of hot/cold water |
| $T^{\mathrm{h,in}}/T^{\mathrm{c,in}}$ | Temperature of inlet hot/cold water |
| $T^{\mathrm{h,out}}/T^{\mathrm{c,out}}$ | Temperature of outlet hot/cold water |
| $m^{\mathrm{h}}/m^{\mathrm{c}}$ | Mass flow rate of hot/cold water |
| $Q^{\mathrm{in}}$ | Heat power delivered to buildings |
| $T^{\mathrm{av}}$ | Average temperature of medium in radiator |
| $T^{\mathrm{air}}/T^{\mathrm{air,ex}}$ | Indoor/outdoor temperature of air |
| $\tau_{ij}/l_{ij}/v_{ij}$ | The transmission delay/length/ mass velocity of the pipeline between node$i$ and node $j$. |
| $T_{ki}$ | Temperature of water flowing from node $k$ to node $i$ at the end of this pipeline |
| $T^{\mathrm{in},k}/T^{\mathrm{out},k}$ | Inlet/outlet temperature of pipeline $k$ |
| $l_k/m_k^w$ | Length/mass flow rate of pipeline $k$ |

| | |
|---|---|
| $Q_1^{\text{loss}}/Q_2^{\text{loss}}/\ Q_3^{\text{loss}}/Q_4^{\text{loss}}$ | Basic/infiltration/invasion/ ventilation heat power loss |
| $g_{\max}^{\text{dec}}/g_{\max}^{\text{inc}}$ | Maximum decreasing/increasing slope of outdoor temperature |
| $t_{\text{c},i}^{\text{dec}}/t_{\text{c},i}^{\text{inc}}$ | Critical time point of heat consumer $i$ |
| $C^{\text{f}}/C^{\text{e}}$ | Costs of fuel/purchased electricity |
| $C^{\text{om}}/C^{\text{WF}}$ | Costs of operation and maintenance/penalty on wind power abandonment |
| $C^{\text{tot}}/\Delta P^{\text{tot}}$ | Total operation cost/power deviation |
| $P_t^{\text{TL,plan}}$ | Planned tie line power at time $t$ |
| $P_k^{\text{g}}/P_k^{\text{d}}$ | Real power of generator injection/load extraction at bus $k$ |
| $\theta_k$ | Voltage phase angle at bus $k$ |
| $B_{kj}$ | Elements of B matrix in DC power flow |
| $Q_i^{\text{d}}/Q_i^{\text{s}}$ | Demand/supply heat at consumer $i$ |

*Parameters:*

| | |
|---|---|
| $P_{\min}^{\text{CHP,r}}/P_{\max}^{\text{CHP,r}}$ | Minimum/maximum ramping limits of the power output of CHP unit |
| $m_{\min}^{\text{s,r}}/m_{\max}^{\text{s,r}}$ | Minimum/maximum ramping limits of the steam mass flow of CHP unit |
| $\mu_1/\mu_2/\mu_3/\ \mu_4/\mu_5/\mu_6$ | Operational coal use coefficient of CHP unit |
| $c^{\text{s}}/c^{\text{w}}$ | Specific heat capacity of steam/water |
| $c^{\text{air}}/c_{\text{p}}^{\text{air,ex}}$ | Specific heat capacity of indoor /outdoor air |
| $T^{\text{phs}}$ | Steam-water phase transition temperature |
| $r^{\text{s}}$ | Unit mass flow latent of steam |
| $K_{\text{S}}^{\text{HX}}/K^{\text{Rad}}/\ K^{\text{env}}$ | Heat transfer coefficient of secondary heat exchanger/ radiator/envelop structure |
| $F_{\text{S}}^{\text{HX}}/F^{\text{Rad}}/\ F^{\text{env}}$ | Effective area for secondary heat exchanger/radiator/ envelop structure |
| $c^{\text{h}}/c^{\text{c}}$ | Specific heat capacity of hot/ cold water |
| $\beta$ | Correction factor for installation positions of radiator |
| $\rho^{\text{air}}/\rho^{\text{air,ex}}$ | Density of indoor/outdoor air |
| $V^{\text{air}}$ | Volume of indoor air |
| $x^{\text{h}}/x^{\text{o}}/$ | Correction factor for height/ orientation |
| $x^{\text{w}}/\gamma$ | Correction factor for wind/ temperature |
| $L^{\text{infil}}/L^{\text{ven}}$ | Volume of cold air infiltration/ventilation |
| $N$ | Number of doors and windows |
| $\eta$ | Ratio of invasion heat loss over basic loss |
| $\tau_k$ | Transmission delay of pipeline $k$ |
| $R$ | Thermal resistance of pipelines |
| $\delta$ | Deviation ratio between supplied and demand heat load |

## I. INTRODUCTION

Combined heat and power (CHP) generation, as an efficient way of energy utilization, has attracted worldwide interest in both academia and industry. The global installed capacity of CHP units has reached 755.2 GW by the end of 2016, among which the Asian-Pacific region and Europe account for 46% and 39%, respectively [1]. In Holland, Finland and Denmark, CHP units have occupied over 60% of the total thermal power units, as well as about 80% of the industrial heating and 30% of the civil heating in China [2].

For one thing promotion of CHP units brings remarkable benefits in improving energy efficiency, for another it reduces the flexibility for system operation due to the strong coupling relationship between heat and power generation, which has been an increasingly highlighted problem since more and more clean power sources with stochastic output characteristics (e.g., wind or solar power plants) are being integrated into the grid at a fast pace. Case in point: in the winter of Northern China, heat demand is high at night but low in daytime, in direct contradiction to the general power output characteristics of wind power plants (WPP). Since CHP units usually operate in the 'heat-led' mode where heat demand is satisfied with higher priority to electric demand, a large amount of electricity is generated at the same time as massive heat is produced to satisfy the high heat demand at night, occupying the room that is reserved for wind power accommodation. As a result, large scale of wind power is curtailed for the sake of secure and stable operation of grid. Statistics from the National Energy Administration show that in China, 41.9 billion kWh wind power has been abandoned in 2017, and the ratio of wind power abandonment in Gansu, Xinjiang, and Jilin Province has reached 33%, 29%, and 21% respectively [3]. It can be seen that how to coordinate the promotion of CHP units with the consumption of wind power has become a critical problem impeding the sustainable development of CHP system.

Researchers have proposed some methods to increase the accommodation of wind power in CHP systems. The most intuitive approach is to equip the system with some electric energy storage (ESS) devices to smooth the power output of WPP [4], [5]. However, large capacity electric storage technology is still at its exploratory stage, and the high investment of building an ESS station is another factor hindering the promotion of such unit at this stage. A preferable way to improve wind power accommodation is to increase the flexibility from heat sector. The feasible operation region of

CHP units is expanded through introducing electric boilers and thermal energy storage (TES) devices, providing extra margin for wind power integration [6]. Heat pump is another widely deployed unit to efficiently convert the excess wind power into heat energy [7]–[10]. Heat pump or electric boiler is usually co-optimized with TES to maximize its capability for wind power accommodation [6], [11], [12]. Compared to ESS, TES is reported to have larger capacity and lower cost [13], thus attracting increasing research interest [14], [15]. A phase-change heat storage facility is introduced into the CHP system to improve adjustability, with which the wind energy loss is reduced from 18.7% to 11.2% [16]. On this basis, a refined phase-change TES model is established considering the heat transfer process, and the performance of such TES device under dynamic working conditions is analyzed [17].

Although the wind power consumption can be significantly improved with electric boilers, heat pumps, and some active TES devices [20], there still exist some thorny problems in applying these units. For example, the extremely low ambient temperature (usually $-20 \sim -30°$ in winter) in northern China has greatly affected the performance of air-source heat pumps. Worse still, excessive installation costs and low usage (typically less than five months a year for electric boilers and TES devices) of these units would remarkably reduce the economical efficiency of the whole system, thus precluding planners from deploying them [21]. For this reason, passive TES devices like the district heating network (DHN) and buildings have received much research attention. The thermal flexibility of buildings is exploited in a combined heat pump and PV panels system to shift the operation of heat pump to periods of PV generation and improve the utilization of on-site PV electricity [22]. A detailed thermal inertia model of the DHN considering the dynamic temperature distribution is proposed for wind power integration, which can also calculate the heat storage rate of DHN quantitatively [23]. A linear CHP dispatch model considering the thermal inertia of both DHN and buildings is constructed, and the performance of the two kinds of thermal inertia in terms of wind power integration is compared [24]. Despite the improved performance reported in these research, the indoor temperature in the building model is usually determined by the supplied thermal power instead of the temperature of supplied hot water, making it difficult to identify the state of heat sector.

Aside from the approaches proposed at physical level, another way to deal with the uncertainty is to implement robust and elaborate strategies at dispatch level. The multi timescale dispatch hierarchy is reported to be an effective measure to reduce the adverse effects of uncertainty on large-scale power system [25], micro-grid [26], and combined cooling, heat and power system [27]–[29]. The idea behind this dispatch method is simple: first divide the dispatch process into several stages (e.g. day-ahead stage and real-time stage) to decompose high level of uncertainty, and then coordinate the objectives of each stage to reduce the effects of uncertainty step by step. Electric power balance requires small timescale control strategies while system economic dispatch needs long time accumulation for global optimization. One of the dominant advantages of this dispatch hierarchy is that a compromise between these two conflicting goals can be achieved in that the requirements of power balance is strictly satisfied in the real-time dispatch and AGC stages, and the goal to obtain higher economical efficiency is reconciled in the day-ahead and intra-day rolling dispatch stages.

Unlike the traditional multi timescale dispatch hierarchy in power systems, CHP systems contain two types of energy flow with totally different transmission characteristics and response rates. Moreover, the supplied and demand thermal power do not have to be balanced in real time due to the influence of building thermal inertia, different from the requirement of real-time power balance in electric sector. Based on the above considerations, adjusting the outputs of heating units (e.g. CHP unit and gas boiler) on a real-time basis is neither necessary nor wise, since frequent adjustment not only increases the complexity for system dispatch but also causes more operation and maintenance (O&M) costs. Therefore, even in the same dispatch stage, heating units should have different dispatch intervals from power units.

Considering the differences in both network side and load side between heat and power sectors, a refined hybrid timescale dispatch hierarchy is proposed in this paper. The thermal inertia of heat sector is also integrated into the dispatch model to improve wind power consumption. The main contributions of this paper include:

1) Some key units and the thermal inertia in CHP systems are modeled, including the transmission delay and heat storage characteristics of DHN, and the storage capacity of buildings. The model of buildings directly links the indoor temperature with the temperature of supplied water, thus can be easily applied to determine the state of heat sector.

2) A hybrid timescale dispatch hierarchy is constructed in this paper, which coordinates the stages of day-ahead dispatch, intraday rolling dispatch, real-time dispatch, and automatic generation control (AGC) to reduce the uncertainty step by step. The thermal inertia is also integrated into the dispatch model to promote wind power accommodation.

3) A practical method for determining the dispatch intervals of each unit is proposed. Considering the extra O&M costs of frequent adjustment, the operation modes of DHN, and the heat storage capacity of buildings, an optimization model is developed to determine the dispatch interval of CHP units.

The rest parts of this paper is organized as follows. In Section II, key units of the CHP system are modeled for further analysis of thermal inertia and dispatch hierarchy. The thermal inertial of heat sector is modeled in Section III. In Section IV, the hybrid timescale dispatch hierarchy is constructed, and the method to determine the dispatch intervals of each unit is discussed in detail. Case studies are conducted to demonstrate the benefits and effectiveness of the proposed method in section V, and the overall work of this paper is concluded in section VI.

## II. MOEDLING KEY UNITS

### A. EXTRACTION TURBINE

CHP unit plays a fundamental role in system operation through generating both electricity and heat from a single fuel source to satisfy the base load. Generally speaking, the steam turbine of a CHP unit can be classified into two types: non-condensing (back-pressure) turbine and extraction turbine. The back-pressure turbine usually operates with a fixed thermoelectric ratio, while the extraction turbine can adjust its electric and thermal power output more flexibly, the operation region of which is shown in Fig. 1.

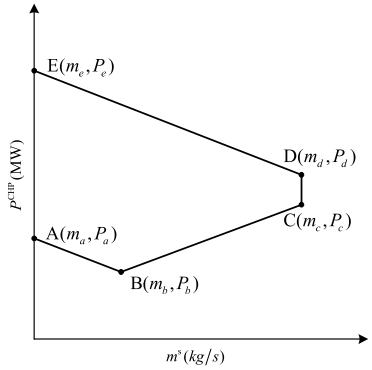


**FIGURE 1.** Operation region of the extraction turbine.

The feasible operation region of an extraction turbine is defined by several extreme operation points and can be formulated as:

$$\begin{cases} P^{\mathrm{CHP}} \geq \dfrac{P_a - P_b}{m_a - m_b}(m^{\mathrm{s}} - m_a) + P_a \\ P^{\mathrm{CHP}} \geq \dfrac{P_b - P_c}{m_b - m_c}(m^{\mathrm{s}} - m_b) + P_b \\ P^{\mathrm{CHP}} \leq \dfrac{P_d - P_e}{m_d - m_e}(m^{\mathrm{s}} - m_d) + P_d \\ m_a \leq m^{\mathrm{s}} \leq m_c \end{cases} \tag{1}$$

Due to the physical constraints of CHP unit and the requirements for stable operation, the electric power output and mass flow rate cannot change arbitrarily, which can be expressed by the ramping up/down constraints in Eq. 2.

$$\begin{cases} P_{\min}^{\mathrm{CHP,r}} \leq P^{\mathrm{CHP}}(t + \Delta t) - P^{\mathrm{CHP}}(t) \leq P_{\max}^{\mathrm{CHP,r}} \\ m_{\min}^{\mathrm{s,r}} \leq m^{\mathrm{s}}(t + \Delta t) - m^{\mathrm{s}}(t) \leq m_{\max}^{\mathrm{s,r}} \end{cases} \tag{2}$$

The operation coal use of CHP unit can be calculated as follows:

$$f^{\mathrm{CHP}}(P^{\mathrm{CHP}}, m^{\mathrm{s}}) = \mu_1 + \mu_2 m^{\mathrm{s}} + \mu_3 P^{\mathrm{CHP}} + \mu_4 (m^{\mathrm{s}})^2 + \mu_5 (P^{\mathrm{CHP}})^2 + \mu_6 m^{\mathrm{s}} \cdot P^{\mathrm{CHP}} \tag{3}$$

### B. HEAT EXCHANGER

The counter-flow heat exchanger is widely used for district heating. Steam-to-water counter-flow heat exchangers are often equipped in the primary heat station to transfer the heat of steam from medium pressure turbine to the water that is pumped into the DHN for district heating, the model of which can be expressed as:

$$\begin{cases} Q_{\mathrm{P}}^{\mathrm{HX}} = c^{\mathrm{s}} m^{\mathrm{s}} (T^{\mathrm{stm}} - T^{\mathrm{phs}}) + r^{\mathrm{s}} m^{\mathrm{s}} \\ Q_{\mathrm{P}}^{\mathrm{HX}} = c^{\mathrm{w}} m^{\mathrm{w}} (T^{\mathrm{w,h}} - T^{\mathrm{w,c}}) \end{cases} \tag{4}$$

Water-to-water counter-flow heat exchangers are often used in the secondary heat station to transfer the heat from primary DHN to secondary one, the model of which can be expressed as:

$$\begin{cases} Q_{\mathrm{S}}^{\mathrm{HX}} = K_{\mathrm{S}}^{\mathrm{HX}} F_{\mathrm{S}}^{\mathrm{HX}} \dfrac{(T^{\mathrm{h,in}} - T^{\mathrm{c,out}}) - (T^{\mathrm{h,out}} - T^{\mathrm{c,in}})}{\ln[(T^{\mathrm{h,in}} - T^{\mathrm{c,out}})/(T^{\mathrm{h,out}} - T^{\mathrm{c,in}})]} \\ \qquad\quad \approx K_{\mathrm{S}}^{\mathrm{HX}} F_{\mathrm{S}}^{\mathrm{HX}} \dfrac{(T^{\mathrm{h,in}} - T^{\mathrm{c,out}}) + (T^{\mathrm{h,out}} - T^{\mathrm{c,in}})}{2} \\ Q_{\mathrm{S}}^{\mathrm{HX}} = c^{\mathrm{c}} m^{\mathrm{c}} (T^{\mathrm{c,out}} - T^{\mathrm{c,in}}) \\ Q_{\mathrm{S}}^{\mathrm{HX}} = c^{\mathrm{h}} m^{\mathrm{h}} (T^{\mathrm{h,in}} - T^{\mathrm{h,out}}) \end{cases} \tag{5}$$

### C. RADIATOR

Radiators are usually installed on the user end to transfer the heat of water from the DHN to the hot air of buildings. The exchanged heat power with a radiator satisfies:

$$\begin{cases} Q^{\mathrm{in}} = K^{\mathrm{Rad}} F^{\mathrm{Rad}} \beta (T^{\mathrm{av}} - T^{\mathrm{air}}) \\ Q^{\mathrm{in}} = c^{\mathrm{w}} m^{\mathrm{w}} (T^{\mathrm{in}} - T^{\mathrm{out}}) \end{cases} \tag{6}$$

In a double-pipe hot water heating system, the radiators of each group are connected in parallel, and the average temperature of heat medium inside the radiator can be determined by Eq. 8.

$$T^{\mathrm{av}} = \frac{T^{\mathrm{in}} + T^{\mathrm{out}}}{2} \tag{7}$$

Bring Eq. 8 into Eq. 7 to eliminate $T^{\mathrm{av}}$ and $T^{\mathrm{out}}$, then we can obtain the exchanged heat power through Eq. 9.

$$Q^{\mathrm{in}} = \frac{K^{\mathrm{Rad}} F^{\mathrm{Rad}} \beta}{1 + \frac{K^{\mathrm{Rad}} F^{\mathrm{Rad}} \beta}{2 c^{\mathrm{w}} m^{\mathrm{w}}}} (T^{\mathrm{in}} - T^{\mathrm{air}}) \tag{8}$$

## III. MODELING THERMAL INERTIA

Thermal inertia of the heat sector is mainly embodied in two aspects: one is the transmission delay and storage characteristics of the DHN, the other is the heat storage capacity of buildings resulting from the allowed variation range of indoor temperature.

### A. THERMAL INERTIA OF THE DHN

With respect to the thermal inertial of DHN, the heat power output of heat source at a certain time is responsible for the heat demand several hours later due to the transmission delay, which means excessive wind energy at night can be converted into heat to serve heat load in daytime. Besides, a hot water DHN under the 'quality regulation' mode can lift its temperature of heat medium to store as much wind energy as possible at night, and release it to supply heat load at other time. The allowed variation range of water temperature makes the DHN act like a storage device to charge/discharge heat

energy, providing additional flexibility for the operation of the whole system.

The transmission delay between two adjacent nodes in the DHN can be calculated by Eq. 10.

$$\tau_{ij} = \frac{l_{ij}}{v_{ij}} \tag{9}$$

The temperature of water flowing through node $i$ can be calculated by:

$$T_i = \frac{1}{\sum_k m_{ki}^{\mathrm{w}}} \sum_k m_{ki}^{\mathrm{w}} \cdot T_{ki}, \quad \forall k \in S^i \tag{10}$$

The storage characteristics is caused by the temperature variation of water in the DHN, which can be expressed as:

$$\begin{cases} T_{\min}^{\mathrm{in},k} \le T^{\mathrm{in},k} \le T_{\max}^{\mathrm{in},k} & \forall k \in S^{\mathrm{p}} \\ T_{\min}^{\mathrm{out},k} \le T^{\mathrm{out},k} \le T_{\max}^{\mathrm{out},k} & \forall k \in S^{\mathrm{p}} \end{cases} \tag{11}$$

Due to the heat dissipation to the environment, the inlet and outlet temperatures of a pipeline satisfy Eq. 13, which can also be viewed as the loss of the DHN acting as a heat storage unit.

$$T^{\mathrm{out},k} = (T^{\mathrm{in},k} - T^{\mathrm{air,ex}}) e^{-\frac{l_k}{R c^{\mathrm{w}} m_k^{\mathrm{w}}}} + T^{\mathrm{air,ex}} \quad \forall k \in S^{\mathrm{p}} \tag{12}$$

### B. THERMAL INERTIA OF BUILDINGS

In terms of the thermal inertial of buildings, indoor temperature can vary within a limited range if only the user comfort is guaranteed, which means the thermal demand of buildings need not be exactly the same as the thermal load. For system operators, the variation range of indoor temperature enables a building to be dispatched as a heat storage unit with limited capacity [21].

Residential heat load consists of three main types of load: heating, hot water, and ventilation. Among them heating load accounts for 80%-90% and has huge potential to regulate. Hence, we focus on the thermal inertia of heating load, more specifically, the thermal inertia of civil buildings, which lies in the allowed variation range of indoor temperature expressed by Eq. 14.

$$T_{\min}^{\mathrm{air}} \le T^{\mathrm{air}}(t) \le T_{\max}^{\mathrm{air}} \tag{13}$$

The indoor temperature also satisfies the following heat transfer equation:

$$Q^{\mathrm{in}} - Q_1^{\mathrm{loss}} - Q_2^{\mathrm{loss}} - Q_3^{\mathrm{loss}} - Q_4^{\mathrm{loss}} = c^{\mathrm{air}} \rho^{\mathrm{air}} V^{\mathrm{air}} \frac{dT^{\mathrm{air}}}{dt} \tag{14}$$

Where

$$\begin{cases} Q_1^{\mathrm{loss}} = (1 + x^{\mathrm{h}}) \sum K^{\mathrm{env}} F^{\mathrm{env}} \gamma (1 + x^{\mathrm{o}} + x^{\mathrm{w}}) \\ \qquad (T^{\mathrm{air}} - T^{\mathrm{air,ex}}) \\ Q_2^{\mathrm{loss}} = 0.28 c_{\mathrm{p}}^{\mathrm{air,ex}} \rho^{\mathrm{air,ex}} L^{\mathrm{infil}} (T^{\mathrm{air}} - T^{\mathrm{air,ex}}) \\ Q_3^{\mathrm{loss}} = N Q_1^{\mathrm{loss,door}} = \eta N Q_1^{\mathrm{loss}} \\ Q_4^{\mathrm{loss}} = 0.28 c_{\mathrm{p}}^{\mathrm{air,ex}} \rho^{\mathrm{air,ex}} L^{\mathrm{ven}} (T^{\mathrm{air}} - T^{\mathrm{air,ex}}) \end{cases} \tag{15}$$

To simplify denotation, let:

$$\begin{cases} \alpha = \dfrac{K^{\mathrm{Rad}} F^{\mathrm{Rad}} \beta}{1 + \frac{K^{\mathrm{Rad}} F^{\mathrm{Rad}} \beta}{2 c^{\mathrm{w}} m^{\mathrm{w}}}} \\ \alpha_1 = (1 + \eta N)(1 + x^{\mathrm{h}}) \sum K^{\mathrm{env}} F^{\mathrm{env}} \gamma \\ \qquad (1 + x^{\mathrm{o}} + x^{\mathrm{w}}) \\ \alpha_2 = 0.28 c_{\mathrm{p}}^{\mathrm{air,ex}} \rho^{\mathrm{air,ex}} (L^{\mathrm{infil}} + L^{\mathrm{ven}}) \\ \alpha_3 = c^{\mathrm{air}} \rho^{\mathrm{air}} V^{\mathrm{air}} \end{cases} \tag{16}$$

Eq. 15 can be rewritten as:

$$\begin{cases} \dfrac{dT^{\mathrm{air}}}{dt} + \dfrac{\alpha + \alpha_1 + \alpha_2}{\alpha_3} T^{\mathrm{air}} = \dfrac{\alpha}{\alpha_3} T^{\mathrm{in}} + \dfrac{\alpha_1 + \alpha_2}{\alpha_3} T^{\mathrm{air,ex}} \\ T^{\mathrm{air}}|_{t=0} = T^{\mathrm{air},0} \end{cases} \tag{17}$$

Since $T^{\mathrm{in}}$ and $T^{\mathrm{air,ex}}$ cannot be analytically expressed, there is no analytical solution to Eq. 18. However, numerical solution can be obtained through Eq. 19.

$$T^{\mathrm{air}}(t) = T^{\mathrm{air},0} e^{-\frac{\alpha+\alpha_1+\alpha_2}{\alpha_3} t} + e^{-\frac{\alpha+\alpha_1+\alpha_2}{\alpha_3} t} \int_0^t \left(\frac{\alpha}{\alpha_3} T^{\mathrm{in}} + \frac{\alpha_1 + \alpha_2}{\alpha_3} T^{\mathrm{air,ex}}\right) e^{\frac{\alpha+\alpha_1+\alpha_2}{\alpha_3} t} \cdot dt \tag{18}$$

The more useful discretized form of the solution is expressed by Eq. 20.

$$\begin{aligned} &T^{\mathrm{air}}(n \cdot \Delta t) \\ &= e^{-\frac{\alpha+\alpha_1+\alpha_2}{\alpha_3} n \cdot \Delta t} \sum_{i=0}^{n} \left(\frac{\alpha}{\alpha_3} T_i^{\mathrm{in}} + \frac{\alpha_1 + \alpha_2}{\alpha_3} T_i^{\mathrm{air,ex}}\right) \cdot e^{\frac{\alpha+\alpha_1+\alpha_2}{\alpha_3} i \cdot \Delta t} \\ &\quad + T^{\mathrm{air},0} e^{-\frac{\alpha+\alpha_1+\alpha_2}{\alpha_3} n \cdot \Delta t}, \quad n = 0, 1, \ldots \end{aligned} \tag{19}$$

## IV. HYBRID TIMESCALE DISPATCH HIERARCHY

### A. CLASSIFICATION OF UNITS

Typical units of a CHP system can be classified into three categories in terms of their response time to dispatch orders: 1) slow response unit, 2) fast response unit, and 3) ultra-fast response unit. Typical units of each category and their features are listed in Tab. 1.

**TABLE 1. Classification of units.**

| Category | Slow response unit | Fast response unit | Ultra-fast response unit |
|---|---|---|---|
| Response time | 0.5 hour ~ several hours | 1 minute ~ 0.5hour | Less than 1 minute |
| Typical units | CHP unit<br>Generator<br>Gas boiler<br>TES device | Electric boiler<br>Heat pump<br>Electric storage<br>WPP<br>Buffer unit | AGC unit<br>Power in tie line |
| Implementation stage | Day-ahead / Intraday rolling dispatch | Intraday rolling / Ultra-short term rolling dispatch | Ultra-short term rolling dispatch / AGC |

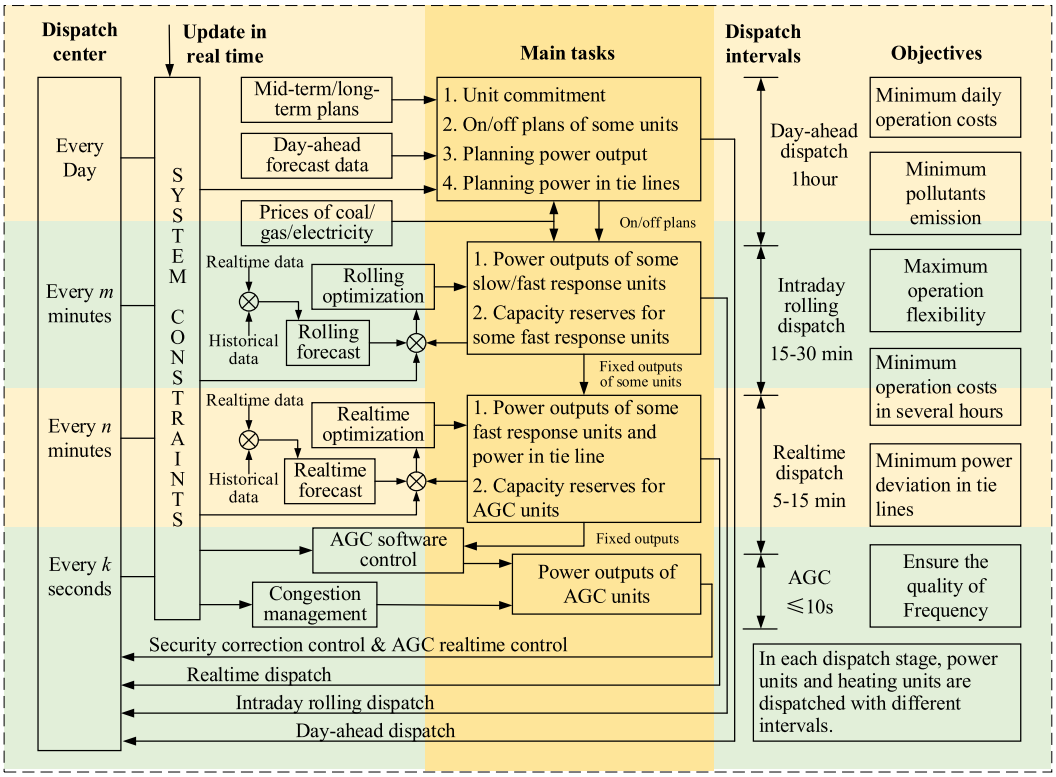


**FIGURE 2.** Hybrid timescale dispatch hierarchy of a CHP system.

### B. DISPATCH HIERARCHY

To reduce the influence of volatility and uncertainty introduced by renewables and loads on a CHP system, a hybrid timescale dispatch hierarchy is established (as is shown in Fig. 2.). Four stages are integrated into the dispatch hierarchy to cooperate with each other, including the day-ahead dispatch, intraday rolling dispatch, real-time dispatch, and automatic generation control (AGC) stage.

In the stage of day-ahead dispatch, unit commitment and on/off plans of some units need to be determined. Besides, the planned power output of each unit and the planned power variation in each tie line are also obtained to provide reference for intraday rolling dispatch. In this stage, dispatch objectives like minimum operation costs, minimum pollutants emission, and maximum operation flexibility are often adopted for global optimization.

As to the stage of intraday rolling dispatch, the actual power outputs of some slow/fast response units are determined with the information of coal/gas/electricity prices, the rolling forecast results of wind power/load, and the day-ahead dispatch plans. Capacity reserves of some fast/ultra-fast response units are also fixed to provide margins for real-time dispatch. Minimizing operation costs in future several hours is a preferred objective in each round of rolling optimization since it can keep a good balance between the requirements of real-time power balance and the global economical efficiency.

Units are usually dispatched every 5 to 15 minutes in the stage of real-time dispatch to further reduce the uncertainty left by previous stages. The power outputs of the rest fast response units and the power variation in each tie line are determined in this stage with the objectives of minimum power deviation from the planned value in tie lines and minimum operation costs in future several hours. Capacity reserves of AGC units are other important outputs of this stage to ensure the proper implementation of the AGC stage.

Quick elimination of potential safety hazards and ensuring the quality of the system frequency are two pivotal goals of the AGC stage. To achieve these goals, correction control and congestion management are implemented in this stage. Correction control uses AGC software and the capacity reserve information to conduct real-time control of AGC units, ensuring the system frequency to meet its requirements. During the process of congestion management, the problem of branch power flow violation is handled in real time so that potential safety threats can be quickly removed without causing any further damage.

### C. METHODS FOR DETERMINING DISPATCH INTERVALS

For power units, the dispatch intervals can be selected according to the common practice [25] as long as the operating constraints of different units are satisfied. For example, 1 hour for the day-ahead dispatch, 15 minutes for the intraday rolling

dispatch, 5 minutes for the real-time dispatch, and 10 seconds for the AGC stage.

However, for heating units, the dispatch intervals can be set to 1 $\sim$ 2 times larger than those of power units under each corresponding dispatch stage since their response time to dispatch orders is generally longer and the thermal power demand need not to be strictly satisfied in real time. Frequently adjusting the outputs of heating units would increase their O&M costs but contribute little to improving the user experience of heating consumers.

Among all the units, large-capacity CHP unit is very crucial in the dispatch hierarchy as it is responsible for the base heating load. If frequently dispatched, its O&M costs would increase remarkably, weakening the overall economical benefits. Contrarily, if scarcely dispatched, serious imbalance between the supplied and demand heat might arise, causing bad heating conditions (e.g. indoor temperature violation). The method to determine the dispatch interval of a large-capacity CHP unit is expatiated as follows.

#### 1) HEATING SYSTEM WITH 'QUANTITY REGULATION' MODE

Under 'quantity regulation' mode, the temperature of heat medium is fixed but the mass flow rate can be adjusted to accommodate varying heat load. Frequently changing the mass flow rate might lead to large-scale pressure fluctuations in the DHN and cause serious accidents like pipeline burst and heating system failure. Therefore, it is better to set the dispatch interval to its maximum value in the premise that the comfort requirements of heating users can be satisfied.

If the outdoor temperature is decreasing, set an initial value of the indoor temperature and assume the outdoor temperature to drop in the worst case:

$$\begin{cases} T^{\text{air},0} = 20°\text{C} \\ T^{\text{in}} = T^{\text{in}}_{\min} \\ T^{\text{air,ex}} = T^{\text{air,ex}}_{\max} - g^{\text{dec}}_{\max} t \end{cases} \tag{20}$$

The underlying logic of this method is to find the maximum time interval that the indoor temperature can remain in its right limit (typically 16$\sim$24° in China) under extreme weather conditions. Increase the time from zero by $\Delta t$ each time until a critical time point $t^{\text{dec}}_{\text{c}}$ that satisfies Eq. 22. is found.

$$\begin{cases} T^{\text{air}}(t^{\text{dec}}_{\text{c}}) \geq T^{\text{air}}_{\min} \\ T^{\text{air}}(t^{\text{dec}}_{\text{c}} + \Delta t) < T^{\text{air}}_{\min} \end{cases} \tag{21}$$

where: $T^{\text{air}}(\cdot)$ is calculated by Eq. 20. $t^{\text{dec}}_{\text{c}}$ in Eq. 22. is the maximum dispatch interval of a CHP unit under such conditions.

If the outdoor temperature is increasing, similarly, set an initial value of the indoor temperature and assume the outdoor temperature to rise in the worst case:

$$\begin{cases} T^{\text{air},0} = 20°\text{C} \\ T^{\text{in}} = T^{\text{in}}_{\max} \\ T^{\text{air,ex}} = T^{\text{air,ex}}_{\min} + g^{\text{inc}}_{\max} t \end{cases} \tag{22}$$

Increase the time from zero by $\Delta t$ each time until a critical time point $t^{\text{inc}}_{\text{c}}$ that satisfies Eq. 24. is found.

$$\begin{cases} T^{\text{air}}(t^{\text{inc}}_{\text{c}}) \leq T^{\text{air}}_{\max} \\ T^{\text{air}}(t^{\text{inc}}_{\text{c}} + \Delta t) > T^{\text{air}}_{\max} \end{cases} \tag{23}$$

$t^{\text{inc}}_{\text{c}}$ in Eq. 24. is the maximum dispatch interval of a CHP unit under this condition.

This method can be generalized to determine the maximum dispatch interval of CHP units in a system with multiple heating consumers. For a CHP system with $n$ heating consumers, the maximum dispatch interval can be obtained by Eq. 25.

$$\Delta t_{\max} = \min \left\{ t^{\text{dec}}_{\text{c},1}, t^{\text{dec}}_{\text{c},2}, \cdots t^{\text{dec}}_{\text{c},n}; t^{\text{inc}}_{\text{c},1}, t^{\text{inc}}_{\text{c},2}, \cdots, t^{\text{inc}}_{\text{c},n} \right\} \tag{24}$$

#### 2) HEATING SYSTEM WITH 'QUALITY REGULATION' MODE

Under 'quality regulation' mode, the mass flow rate of heat medium is fixed but the temperature of supplied water can be adjusted. Since hydraulic imbalance of the DHN rarely occurs under such operation mode, we can focus on the influence of different dispatch intervals on the system economical efficiencies and select an optimal dispatch interval with minimum operation costs.

First of all, the dispatch interval should be within a limit expressed by Eq. 26.

$$\Delta t_{\min} \leq \Delta t \leq \Delta t_{\max} \tag{25}$$

where: $\Delta t_{\min}$ is the minimum dispatch interval determined by the operation constraints of CHP units; $\Delta t_{\max}$ is the maximum dispatch interval calculated by Eq. 25.

After that, in the stage of day-ahead dispatch, take minimum daily operation costs of the whole system as the dispatch objective and set the dispatch intervals of CHP units to be the following values:

$$\Delta t = \varepsilon_{\min} \Delta t^{\text{I}}, (\varepsilon_{\min} + 1)\Delta t^{\text{I}}, \ldots, (\varepsilon_{\max} - 1)\Delta t^{\text{I}} \tag{26}$$

where: $\Delta t^{\text{I}}$ is the dispatch interval of power units in the stage of day-ahead dispatch; coefficients $\varepsilon_{\min}$ and $\varepsilon_{\max}$ characterize the minimum and maximum dispatch intervals, and can be calculated by Eq. 28.

$$\begin{cases} \varepsilon_{\min} = ceil(\Delta t_{\min}/\Delta t^{\text{I}}) \\ \varepsilon_{\max} = ceil(\Delta t_{\max}/\Delta t^{\text{I}}) \end{cases} \tag{27}$$

where: $ceil(\cdot)$ is the function to get the minimum integer that larger than the input.

Next, take one dispatch interval each time from Eq. 27. and solve the optimal day-ahead dispatch model to get the corresponding daily operation cost. The optimal dispatch interval is the one when the daily operation cost reaches its minimum. The procedures of determining the optimal dispatch interval of a CHP unit are illustrated in Fig. 3.

## V. CASE STUDY

In this section, the configuration of the case CHP system is first sketched. Then the potential of reducing operation costs and improving wind power consumption with the thermal

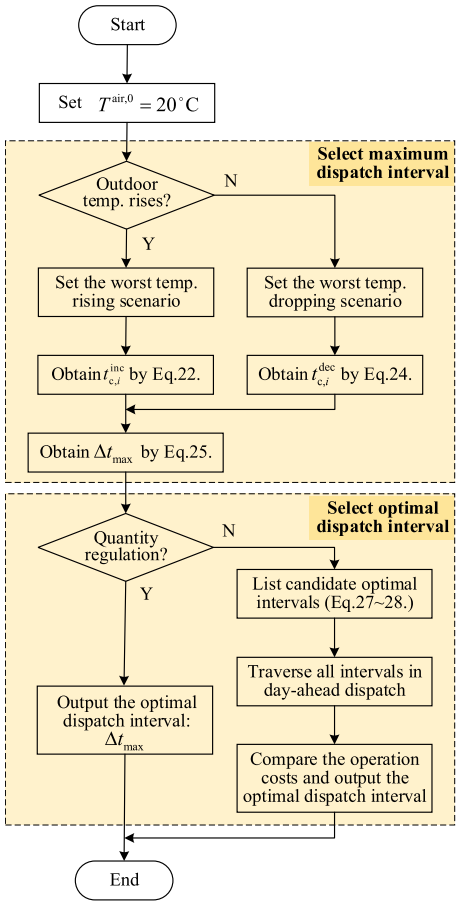


**FIGURE 3.** Flow chart of determining dispatch intervals of CHP units.

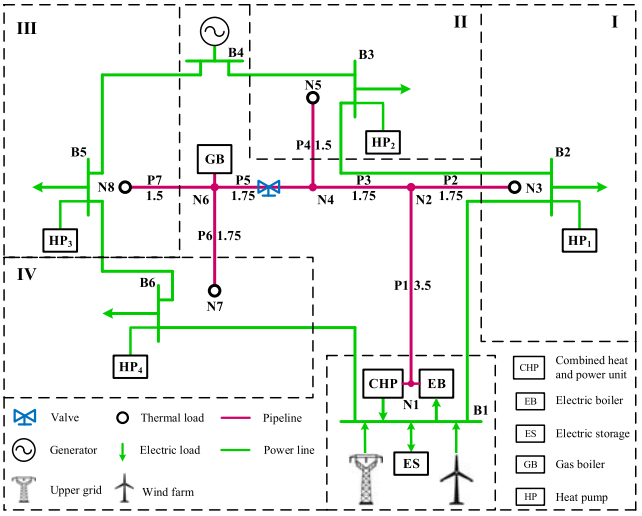


**FIGURE 4.** Layout of the CHP system in the case study.

**TABLE 2.** Dispatch interval of each unit.

| Unit | Day-ahead dispatch | Intraday rolling dispatch | Real-time dispatch | AGC stage |
|---|---|---|---|---|
| CHP unit | 3 hours | 3 hours | × | × |
| Generator | 1 hour | 15 minutes | × | × |
| Gas boiler | 1 hour | 30 minutes | × | × |
| Heat pump | 1 hour | 15 minutes | × | × |
| WPP | 1 hour | 15 minutes | 5 minutes | × |
| Electric boiler | 1 hour | 15 minutes | 5 minutes | × |
| Electric storage | 1 hour | 15 minutes | 5 minutes | × |
| Buffer unit | × | × | 5 minutes | × |
| Tie line | 1 hour | 15 minutes | 5 minutes | × |
| AGC unit | × | × | × | 10 seconds |

inertia of heat sector is validated through comparisons among four different cases. After that, results of the hybrid timescale dispatch hierarchy are displayed to further confirm the feasibility and effectiveness of the proposed dispatch method. The parameters and data of the case study are based on a real CHP system (detailed in [29]) in Jilin Province, China.

### A. CONFIGURATION OF THE CASE SYSTEM

The layout of the primary heating network is shown in Fig. 4, which covers 14 pipelines, 16 nodes and 4 secondary heat exchangers. Two heat sources are located in this area: one is the CHP plant with a peak shaving electric boiler, the other is an independent gas boiler connected to node 6. A WPP and ESS share the same 110 kV transmission bus with CHP plant and electric boiler to provide as smooth wind power as possible. The CHP system is connected with another power system through a bidirectional tie line. The load is divided into four parts based on geographic location, and each load center is equipped with a heat pump unit.

The dispatch interval of each unit is listed in Tab. 2, where '×' means one unit is not dispatched in the corresponding stage. According to the method proposed in Part IV, when the dispatch interval of the CHP unit is set to be 3 hours, minimum daily operation costs can be achieved.

All tests are run on an Intel(R) Core(TM) i7-7700HQ CPU @ 2.80GHz personal computer with 16.0 GB memory. Programs are coded using MATLAB® and solved by toolbox YALMIP with solver CPLEX 12.8.0.

### B. COMPARISONS OF DAILY OPERATION COSTS AND WIND POWER CONSUMPTION

In order to demonstrate the impact of thermal inertia on reducing operation costs and improving wind power accommodation, four cases are simulated for comparison. Case 1 is an ordinary case without considering the thermal inertia of DHN and buildings. Case 2 only considers that of buildings, and Case 3 only considers that of DHN. Case 4 is the proposed method that takes into account the thermal inertia of both DHN and buildings. The optimization results of day-ahead dispatch in terms of daily operation costs are shown in Tab. 3, where $C^{f+om}$ is the sum of fuel costs and O&M costs. The total daily operation cost of case 2 has reduced $6.6 \times 10^3$ \$ per day compared to case 1, and that of case 3 and case 4 are $1.53 \times 10^4$ \$ and $1.75 \times 10^4$ \$ respectively, which demonstrates the potential of improving system economical efficiency with the thermal inertial of heat sector. The decrease

**TABLE 3.** Cost comparison among four cases ($\times 10^5$ \$).

| Case | Building | DHN | $C^{\mathrm{f+om}}$ | $C^{\mathrm{e}}$ | $C^{\mathrm{WF}}$ | $C^{\mathrm{tot}}$ |
|---|---|---|---|---|---|---|
| 1 | × | × | 4.136 | -0.053 | 0.051 | 4.134 |
| 2 | √ | × | 4.073 | -0.053 | 0.048 | 4.068 |
| 3 | × | √ | 3.990 | -0.053 | 0.044 | 3.981 |
| 4 | √ | √ | 3.970 | -0.053 | 0.042 | 3.959 |

on penalty costs of abandoned wind power from case 1 to case 4 proves that the storage characteristics of buildings and DHN can enable the system to consume more wind power.

Fig. 5(a) shows the wind power consumption of all cases, from which we can see that during 05:00 ∼ 19:00, the wind power is nearly all absorbed in four cases. However, during 00:00 ∼ 05:00 and 19:00 ∼ 22:00, when the wind power is oversupplied, curtailment occurs in all cases. However, the amount of curtailed wind power is reduced by integrating the thermal inertia into the dispatch process (as is shown in case 2, 3, and 4). The discarding rate of wind power drops from 8.79% to 7.33% (see Fig. 5(b)) when considering the thermal inertia, further verifying the capability of thermal inertia to improve wind power accommodation. In this case, the thermal inertia of DHN has better performance than that of buildings since the former reduces the discarding rate by 1.32% while the later just 0.67%.

### C. RESULTS OF THE HYBRID TIMESCALE DISPATCH

In our case study, unit commitment and on/off plans of the ESS are determined in the stage of day-ahead dispatch with the objective of minimum daily operation costs. The actual power outputs of CHP unit, generator, gas boiler and heat pumps are rolling optimized with the objective of minimum operation costs in the future 6 hours in the stage of intraday rolling dispatch. The actual power outputs of electric boiler, ESS, buffer unit and the power variation in tie line are determined with the objective of minimum tie line power deviation from the planned value in the future 2 hours in the stage of real-time dispatch. The objectives in each dispatch stage are formulated in Eq. 29.

$$\begin{cases} \min C^{\mathrm{tot}} = \sum_{t=1}^{24} C_t^{\mathrm{f}} + C_t^{\mathrm{e}} + C_t^{\mathrm{om}} + C_t^{\mathrm{WF}} \\ \min C_j^{\mathrm{tot}} = \sum_{t=j}^{j+24} C_t^{\mathrm{f}} + C_t^{\mathrm{e}} + C_t^{\mathrm{om}} + C_t^{\mathrm{WF}}, \\ \qquad j = 1, 2, \cdots 72 \\ \min \left| \Delta P_j^{\mathrm{tot}} \right| = \sum_{t=j}^{j+24} \left| P_t^{\mathrm{TL}} - P_t^{\mathrm{TL,plan}} \right|, \\ \qquad j = 1, 2, \cdots 264 \end{cases} \tag{28}$$

Constraints of power grid are expressed in the DC power flow formulation. Due to the thermal inertia of buildings, the system can operate in the condition that the supplied and demand heat power are slightly mismatched, but the total heat

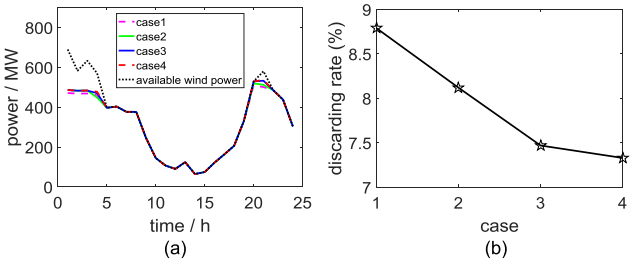


**FIGURE 5.** Contrast of wind power consumption among four cases.

supplied within six hours should equal to the total demand within this period, which can be formulated as:

$$\begin{cases} (1-\delta)Q_i^{\mathrm{d}} \le Q_i^{\mathrm{s}} \le (1+\delta)Q_i^{\mathrm{d}} \\ \sum_t \sum_i Q_{i,t}^{\mathrm{s}} = \sum_t \sum_i Q_{i,t}^{d}, \quad \forall i \in S^{\mathrm{load}} \end{cases} \tag{29}$$

In summary, the dispatch model in each stage is a mixed integer quadratic programming (MIQP) problem since the objective function contains both linear and quadratic components, and the constraints contain both linear and integer components.

#### 1) OVERALL DISPATCH RESULTS OF THE ELECTRIC AND HEAT SECTOR

Dispatch results of three stages (day-ahead, intraday rolling, and real-time) in both electric and heat sector are displayed in Fig. 6. Since the electric demand is balanced in real time, the actual outputs of all power units (see the dotted black line in Fig. 6(a)) approximately equal to the power demand. From Fig. 6(a), we can see the accuracy of tracking the power load increases step by step from day-ahead dispatch (see the black line with triangles) to intraday rolling dispatch (see the red line with crosses), and finally to real-time dispatch (see the blue line with circles), which demonstrates that the proposed hybrid timescale dispatch hierarchy can gradually reduce the uncertainty and volatility introduced by loads and renewables, further ensuring the safe and stable operation of the whole CHP system.

As is shown in Fig. 6(b), dispatch results in heat sector have much greater deviation from the demand than those in electric sector due to the thermal inertia of buildings. Despite the mismatch between supplied and demand thermal power at some time, the indoor temperature can still remain in acceptable limits as long as the supplied and demand heat are balanced within a suitable period. The thermal power output in day-ahead dispatch deviates greater from the thermal demand compared to that in intraday rolling dispatch, but the real-time dispatch further improves the performance in that the thermal power output fluctuates closely around the load curve without causing long time imbalance, which further validates the feasibility and effectiveness of the proposed dispatch method.

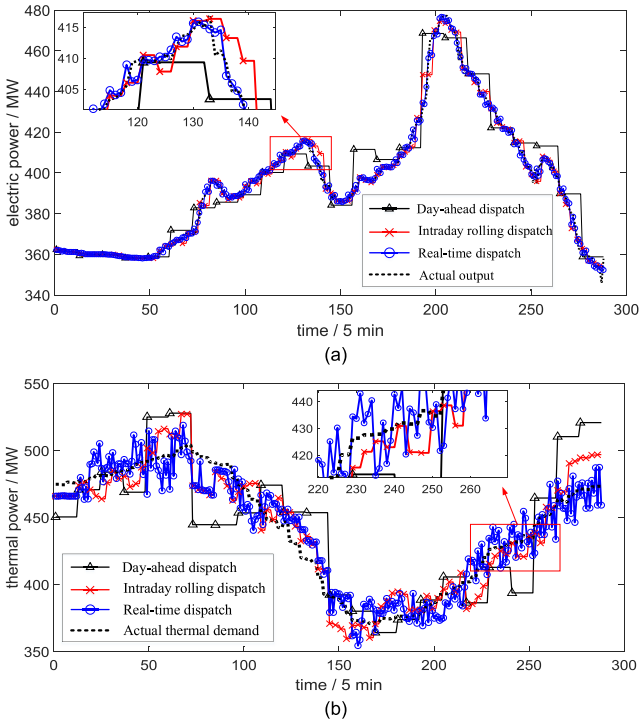


**FIGURE 6.** Dispatch results of three stages in electric and heat sector. (a) Electric sector. (b) Heat sector.

### 2) DISPATCH RESULTS OF DIFFERENT UNITS

The real-time dispatch results of heating units are shown in Fig. 7(a). During the peak-hour of wind power generation, the heat pumps and electric boiler make good use of the excessive wind power to produce as much heat as possible. Low electric demand limits the thermal power output of CHP unit, and the rest thermal demand needs to be satisfied by gas boiler. When the wind power is very rare at noon, the CHP unit has to raise its thermal power output, but the heat pumps and electric boiler tend to reduce their outputs. It is worth noting that the deviation between forecast thermal load (see the red line in Fig. 7(a)) and supplied thermal power (see the blue line in Fig. 7(a)) is due to the thermal inertia of heat sector, and that between supplied thermal power and total thermal power output is caused by the transmission delay and transmission loss of the DHN.

The real-time dispatch results of electric units and WPP are displayed in Fig. 7(b). The red line represents the sum of system electric load and the power consumed by electric boiler and heat pumps. When the wind power is superfluous, excessive electricity is delivered out or stored in the ESS. In the opposite case, the system needs to purchase power through the tie line, and the ESS will discharge to meet the electric load. The buffer unit fast adjust its power output to smooth the power fluctuations in tie line, the results of which are shown in Fig. 7(c). The maximum power deviation in tie line between the actual (blue line) and planned value (red line) is no more than 20 MW, and the period at which deviation occurs is limited to several hours, demonstrating the good performance of the proposed method.

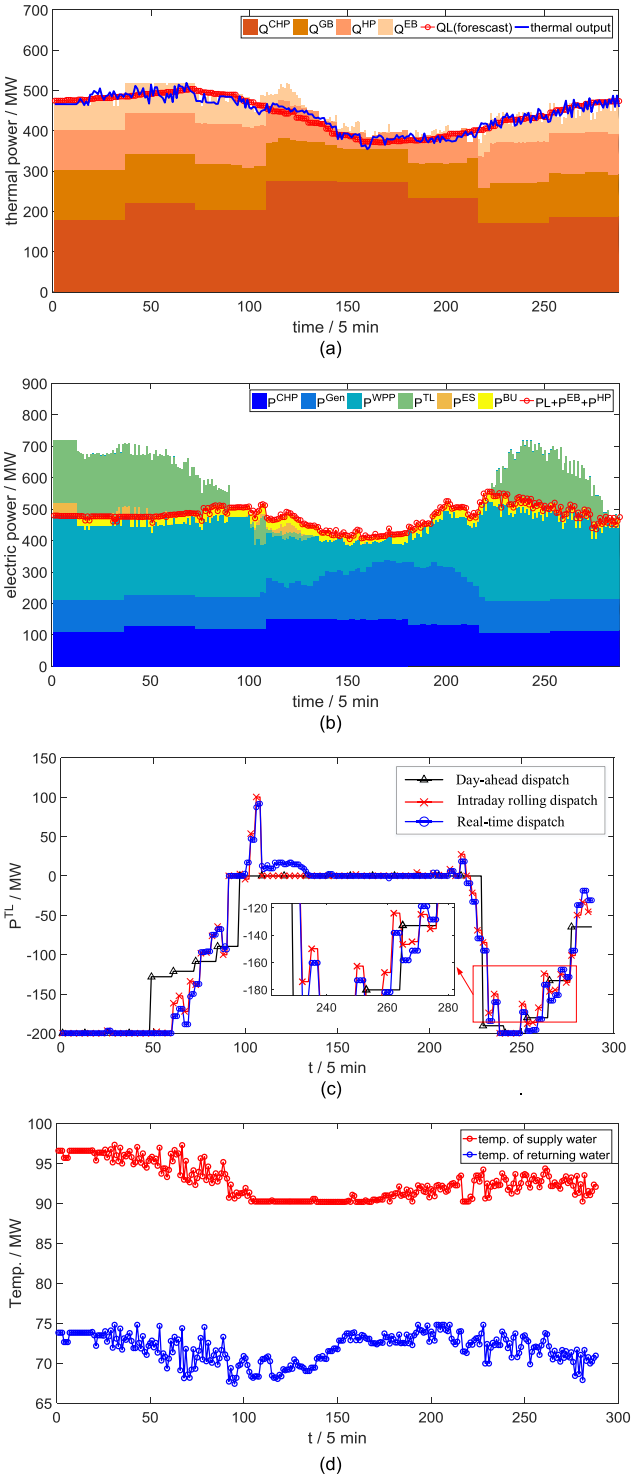


**FIGURE 7.** Dispatch results of different units. (a) Real-time dispatch results of heating units. (b) Real-time dispatch results of electric units and WPP. (c) Dispatch results of power variation in the tie line. (d) Temperatures of supply and returning water at node 4.

The temperatures of supply and returning water at node 4 are displayed in Fig. 7 (d), from which we can see that the supply water temperature fluctuates up and down within a small range at 93°, while the returning water temperature

fluctuates at 72°, in accordance with the rated 95-70° operation conditions. The temperature of supply water is elevated to store the extra wind energy at peak wind power hours, and lowered to release the stored energy at valley ones. The temperature of returning water is determined by both the temperature of supply water and the thermal demand, so it remains at a high level from 12:30 to 17:00 as the low level of thermal demand plays a superior role to the scarce wind power output during this period.

## VI. CONCLUSION

A hybrid timescale dispatch hierarchy is proposed to better accommodate the uncertainty of CHP system in this paper, where heating units have different scheduling intervals from power units in each dispatch stage due to the different features of heat and power. The method to determine the scheduling intervals of each unit is also discussed in detail. Moreover, the thermal inertia of heat sector is integrated into the dispatch model to improve wind power consumption. Results of case study demonstrate the feasibility and effectiveness of proposed dispatch method in dealing with the uncertainty introduced by renewables and loads.

In fact, the basic connotation of the proposed hybrid timescale dispatch hierarchy is not limited to different dispatch intervals for heating and power units. Selection of non-constant dispatch interval of each unit according to the forecast of load and renewables profiles is another issue worthy of further investigation. In addition, different sampling periods of heat sector and different rolling forecast horizons in the stage of rolling dispatch all have their own contradictions between computational complexity and simulation accuracy. Techniques to select the optimal sampling period and optimal rolling forecast horizon require further research.

## REFERENCES


[1] Polaris Power Grid. *Analysis of Global Cogeneration Development*. Accessed: Jun. 25, 2018. [Online]. Available: http://news.bjx.com.cn/html/20180625/908255.shtml

[2] China Market Research Online. *Investigation and forecastof China's cogeneration industry in 2017–2023*. Accessed: Aug. 20, 2018. [Online]. Available: http://www.cninfo360.com/yjbg/nyhy/qt/20170313/541142.html

[3] The National Energy Administration. *Statistics of Wind Power in 2017*. Accessed: Feb. 1, 2018. [Online]. Available: http://www.nea.gov.cn/2018-02/01/c_136 942234.htm

[4] F. Luo, K. Meng, Z. Y. Dong, Y. Zheng, Y. Chen, and K. P. Wong, "Coordinated operational planning for wind farm with battery energy storage system," *IEEE Trans. Sustain. Energy*, vol. 6, no. 1, pp. 253–262, Jan. 2015.

[5] R. Yuan, J. Ye, J. Lei, and T. Li, "Integrated combined heat and power system dispatch considering electrical and thermal energy storage," *Energies*, vol. 9, no. 6, pp. 474–491, Jun. 2016.

[6] X. Chen *et al.*, "Increasing the flexibility of combined heat and power for wind power integration in China: Modeling and implications," *IEEE Trans. Power Syst.*, vol. 30, no. 4, pp. 1848–1857, Jul. 2015.

[7] T. Capuder and P. Mancarella, "Techno-economic and environmental modelling and optimization of flexible distributed multi-generation options," *Energy*, vol. 71, pp. 516–533, Jul. 2014.

[8] M. G. Nielsen, J. M. Morales, M. Zugno, T. E. Pedersen, and H. Madsen, "Economic valuation of heat pumps and electric boilers in the Danish energy system," *Appl Energy*, vol. 167, pp. 189–200, Apr. 2016.

[9] S. Sichilalu, T. Mathaba, and X. Xia, "Optimal control of a wind–PV-hybrid powered heat pump water heater," *Appl Energy*, vol. 185, pp. 1173–1184, Jan. 2016.

[10] L. Hongyu, F. Lin, and X. Ruilin, "Research on the electric grid dispatch for alleviating the uncertainties impact through gas-fired cogenerations and heat pumps," *Trans. China Electro-Tech. Soc.*, vol. 30, no. 20, pp. 219–226, Sep. 2015.

[11] Y. Yang, K. Wu, X. Yan, J. Gao, and H. Long, "The large-scale wind power integration using the integrated heating load and heating storage control," presented at the IEEE Eindhoven PowerTech, Eindhoven, The Netherlands, 2015.

[12] H. Lund, "Large-scale integration of wind power into different energy systems," *Energy*, vol. 30, no. 13, pp. 2402–2412, Oct. 2005.

[13] S. Kuravi, J. Trahan, D. Y. Goswami, M. M. Rahman, and E. K. Stefanakos, "Thermal energy storage technologies and systems for concentrating solar power plants," *Prog. Energy Combustion Sci.*, vol. 39, no. 4, pp. 285–319, Aug. 2013.

[14] H. Ma *et al.*, "A dispatch method of combined heat and power plants with heat storage facilities for wind power accommodation," presented at the 6th ICRERA, San Diego, CA, USA, Nov. 2017.

[15] Y. Dai *et al.*, "A general model for thermal energy storage in combined heat and power dispatch considering heat transfer constraints," *IEEE Trans. Sustain. Energy*, vol. 9, no. 4, pp. 1518–1528, Oct. 2018. [Online]. Available: https://ieeexplore.ieee.org/document/8259014/

[16] K. Hu *et al.*, "Phase-change heat storage installation in combined heat and power plants for integration of renewable energy sources into power system," *Energy*, vol. 124, pp. 640–651, Apr. 2017.

[17] Y. Dai *et al.*, "Integrated dispatch model for combined heat and power plant with phase-change thermal energy storage considering heat transfer process," *IEEE Trans. Sustain. Energy*, vol. 9, no. 3, pp. 1234–1243, Jul. 2018.

[18] T. Fang and R. Lahdelma, "Optimization of combined heat and power production with heat storage based on sliding time window method," *Appl. Energy*, vol. 162, pp. 723–732, Jan. 2016.

[19] H. Wang, W. Yin, E. Abdollahi, R. Lahdelma, and W. Jiao, "Modelling and optimization of CHP based district heating system with renewable energy production and energy storage," *Appl. Energy*, vol. 159, no. 1, pp. 401–421, Dec. 2015.

[20] Y. Dai *et al.*, "Active and passive thermal energy storage in combined heat and power plants to promote wind power accommodation," *J. Energy Eng.*, vol. 143, no. 5, p. 04017037, Oct. 2017.

[21] W. Gu, J. Wang, S. Lu, Z. Luo, and C. Wu, "Optimal operation for integrated energy system considering thermal inertia of district heating network and buildings," *Appl. Energy*, vol. 199, pp. 234–246, Aug. 2017.

[22] A. Toradmal, T. Kemmler, and B. Thomas, "Boosting the share of onsite PV-electricity utilization by optimized scheduling of a heat pump using buildings thermal inertia," *Appl. Therm. Eng.*, vol. 137, pp. 248–258, Jun. 2018.

[23] J. Zheng, Z. Zhou, J. Zhao, and J. Wang, "Integrated heat and power dispatch truly utilizing thermal inertia of district heating network for wind power integration," *Appl. Energy*, vol. 211, pp. 865–874, Feb. 2018.

[24] L. Zhang and Y. Luo, "Combined heat and power scheduling: Utilizing building-level thermal inertia for short-term thermal energy storage in district heat system," *IEEJ Trans. Elect. Electron. Eng.*, vol. 13, no. 6, pp. 804–814, Jun. 2018.

[25] B. Zhang, W. Wu, T. Zheng, and H. Sun, "Design of a multi-time scale coordinated active power dispatching system for accommodating large scale wind power penetration," *Autom. Electr. Power Syst.*, vol. 35, no. 1, pp. 1–6, Jan. 2011.

[26] H. Qiu, W. Gu, Y. Xu, and B. Zhao, "Multi-time-scale rolling optimal dispatch for AC/DC hybrid microgrids with day-ahead distributionally robust scheduling," *IEEE Trans. Sustain. Energy*, to be published. Accessed: Sep. 3, 2018, doi: 10.1109/.TSTE.2018.2868548.

[27] Z. Bao, Q. Zhou, Z. Yang, Q. Yang, L. Xu, and T. Wu, "A multi time-scale and multi energy-type coordinated microgrid scheduling solution—Part I: Model and methodology," *IEEE Trans. Power Syst.*, vol. 30, no. 5, pp. 2257–2266, Sep. 2015.

[28] W. Gu, Z. Wang, Z. Wu, Z. Luo, Y. Tang, and J. Wang, "An online optimal dispatch schedule for CCHP microgrids based on model predictive control," *IEEE Trans. Smart Grid*, vol. 8, no. 5, pp. 2332–2342, Sep. 2017.

[29] (2018). *Test Data for Hybrid Timescale Dispatch Hierarchy for the Combined Heat and Power System Considering the Thermal Inertia of Heat Sector*. [Online]. Available: https://pan.baidu.com/s/1Gb9nlfaOMJbDRAsVB9yiaQ

**SHUAI YAO** received the B.S. degree in electrical engineering from the Honors College of Nanjing Normal University, China, in 2017.

He is currently pursuing the Ph.D. degree in electrical engineering of Southeast University.

**WEI GU** received the B.S. and Ph.D. degrees in electrical engineering from Southeast University, Nanjing, China, in 2001 and 2006, respectively.

From 2009 to 2010, he was a Visiting Scholar with the Department of Electrical Engineering, Arizona State University, Tempe, AZ, USA. He is currently a Professor with the School of Electrical Engineering, Southeast University. His research interests include distributed generations and microgrids, active distribution networks, and integrated energy system.

**SUYANG ZHOU** received the B.S. degree in electrical engineering from the Huazhong University of Science and Technology in 2009 and the Ph.D. degree in electrical engineering from the University of Birmingham in 2015. He is currently a Lecturer with the School of Electrical Engineering, Southeast University.

He was a KTP Associate with the University of Leicester. His main research interests include integrated energy system, big data, and demand side management.

**SHUAI LU** received the B.S. degree in smart grid information engineering from the School of Automation, Nanjing University of Science and Technology, China, in 2016.

He is currently pursuing the Ph.D. degree in electrical engineering with Southeast University.

**CHENYU WU** received the B.S. degree in electrical engineering from Hohai University, China, in 2015.

He is currently pursuing the Ph.D. degree in electrical engineering with Southeast University.

**GUANGSHENG PAN** received the B.S. and M.S. degrees in electrical engineering from Shandong University, China, in 2014 and 2017, respectively.

He is currently pursuing the Ph.D. degree in electrical engineering with Southeast University.